STEM CELLS®

TRANSLATIONAL AND CLINICAL RESEARCH

Adipose-Derived Mesenchymal Stem Cells Ameliorate Chronic Experimental Autoimmune Encephalomyelitis

GABRIELA CONSTANTIN,[a] SILVIA MARCONI,[b] BARBARA ROSSI,[a] STEFANO ANGIARI,[a] LAURA CALDERAN,[c] ELENA ANGHILERI,[b] BEATRICE GINI,[b] SIMONE DOROTHEA BACH,[a] MARIANNA MARTINELLO,[a] FRANCESCO BIFARI,[d] MIRCO GALIÈ,[c] ERMANNA TURANO,[b] SIMONA BUDUI,[a] ANDREA SBARBATI,[c] MAURO KRAMPERA,[d] BRUNO BONETTI[b]

[a]Department of Pathology, Section of General Pathology; and [c]Department of Morphological-Biomedical Sciences, Section of Anatomy, University of Verona, Italy; [b]Department of Neurological Sciences and Vision, Section of Neurology; [d]Department of Clinical and Experimental Medicine, Section of Haematology, University of Verona, Policlinico G.B. Rossi, Verona, Italy

Key Words. Adipose-derived mesenchymal stem cells • Chronic experimental autoimmune encephalomyelitis • Immune regulation • Neural precursors • T lymphocytes • Imaging, in vivo • Growth factors

ABSTRACT

Mesenchymal stem cells (MSCs) represent a promising therapeutic approach for neurological autoimmune diseases; previous studies have shown that treatment with bone marrow-derived MSCs induces immune modulation and reduces disease severity in experimental autoimmune encephalomyelitis (EAE), an animal model of multiple sclerosis. Here we show that intravenous administration of adipose-derived MSCs (ASCs) before disease onset significantly reduces the severity of EAE by immune modulation and decreases spinal cord inflammation and demyelination. ASCs preferentially home into lymphoid organs but also migrates inside the central nervous system (CNS). Most importantly, administration of ASCs in chronic established EAE significantly ameliorates the disease course and reduces both demyelination and axonal loss, and induces a Th2-type cytokine shift in T cells. Interestingly, a relevant subset of ASCs expresses activated α4 integrins and adheres to inflamed brain venules in intravital microscopy experiments. Bioluminescence imaging shows that α4 integrins control ASC accumulation in inflamed CNS. Importantly, we found that ASC cultures produce basic fibroblast growth factor, brain-derived growth factor, and platelet-derived growth factor-AB. Moreover, ASC infiltration within demyelinated areas is accompanied by increased number of endogenous oligodendrocyte progenitors. In conclusion, we show that ASCs have clear therapeutic potential by a bimodal mechanism, by suppressing the autoimmune response in early phases of disease as well as by inducing local neuroregeneration by endogenous progenitors in animals with established disease. Overall, our data suggest that ASCs represent a valuable tool for stem cell–based therapy in chronic inflammatory diseases of the CNS. STEM CELLS *2009;27:2624–2635*

Disclosure of potential conflicts of interest is found at the end of this article.

INTRODUCTION

Multiple sclerosis (MS) and its animal model, the experimental autoimmune encephalomyelitis (EAE), are autoimmune disorders targeting the central nervous system (CNS), where the inflammatory response leads to demyelination [1]. In both diseases, axonal pathology occurs in the early phase, correlates with inflammation, and critically contributes to disease severity [1–3]. Thus, chronic EAE is a suitable model to test therapeutic approaches that simultaneously target both inflammation and neurodegeneration. In this regard, neural precursor cells (NPCs) were the first candidates for cell-based therapy in neuroinflammation because of their capacity for cell replacement in chronic EAE and their local and systemic immune modulatory effects in relapsing EAE [4, 5]. In fact, NPCs were effective when injected after disease stabilization in chronic EAE animals by promoting neuroregeneration through a supportive effect on endogenous progenitors [4]. The homing of NPCs into the CNS was dependent on integrin

Author contributions: G.C.: Conception and design, final approval of manuscript, financial support, manuscript writing; S.M.: Data analysis and interpretation; B.R.: Data analysis and interpretation; S.A.: Data analysis and interpretation; L.C.: Data analysis and interpretation; E.A.: Data analysis and interpretation; B.G.: Data analysis and interpretation; S.D.B.: Data analysis and interpretation; M.M.: Data analysis and interpretation; F.B.: Provision of study material, collection, and/or assembly of data; M.G.: Provision of study material, collection, and/or assembly of data; E.T.: Data analysis and interpretation; S.B.: Data analysis and interpretation; A.S.: Conception and design, manuscript writing; M.K.: Conception and design, final approval of manuscript, financial support; B.B.: Conception and design, final approval of manuscript, financial support, manuscript writing.

Correspondence: Bruno Bonetti, M.D., Ph.D., Associate Professor in Neurology, Section of Clinical Neurology, Department of Neurological Sciences and Vision, University of Verona, P. le L.A. Scuro 10, 37134 Verona, Italy. Telephone: +39-045-8124694; Fax: +39-045-8027492; e-mail: bruno.bonetti@univr.it; or Gabriela Constantin, M.D., Ph.D., Assistant Professor of Pathology, Section of General Pathology, Department of Pathology, University of Verona, Strada le Grazie 8, 37134 Verona, Italy. Telephone: +39-045-8027102; Fax: +39-045-8027127; e-mail: gabriela.constantin@univr.it Received May 20, 2009; accepted for publication August 1, 2009; first published online in STEM CELLS *EXPRESS* August 12, 2009. 1066-5099/2009/$30.00/0 doi: 10.1002/stem.194

VLA-4, the counter-ligand for endothelial vascular cell adhesion molecule-1 (VCAM-1) [5].

However, the invasiveness associated with harvesting NPCs and the reduced number of cells that can be obtained may limit their clinical application. As the efforts to bring experimental advances to the clinic are mounting, the source of these cells is becoming a crucial issue. A potential alternative to NPCs is represented by mesenchymal stem cells (MSCs) (also named multipotent stromal cells) [6], a subset of adult stem cells present in virtually all tissues, including bone marrow (BM), adipose tissue, umbilical cord blood, and dermis [7–9]. MSCs can differentiate in vitro into multiple mesenchymal and nonmesenchymal lineages and can efficiently induce the proliferation, migration, and differentiation of neural endogenous progenitors through the secretion of neural growth factors, thus representing an attractive therapy for regenerative medicine [10]. In addition, MSCs have relevant immune modulatory effects both in vivo and in vitro, as they can suppress many functions of immune cells [11–14]. This feature makes MSCs suitable for the therapy of autoimmune diseases. Indeed, mouse BM-derived MSCs (BM-MSCs) have been shown to ameliorate chronic and relapsing EAE [15–19] by inhibiting Th1 T cells and modulating Th17-polarized response [13, 20]. However, the beneficial effect was evident only when BM-MSCs were injected before or at the onset of disease; they were unable to cure established disease [15]. More recently, human BM-MSCs have been shown not only to induce Th2-shift of the immune response, but also to promote endogeneous repair in chronic EAE [19]. However, the mechanisms of BM-MSC contribution to neuroregeneration in chronic EAE are not clearly understood. In fact, murine BM-MSCs do not express α4 integrins [21], and the study of BM-MSC homing in EAE lesions has provided conflicting results regarding the capacity of BM-MSCs to migrate into the inflamed CNS [15–19].

Much attention has been paid recently to adipose-derived MSCs (ASCs) because adipose tissue is an abundant, easily accessible, and appealing source of donor tissue for autologous cell transplantation [22, 23]. Several groups have demonstrated that ASCs display multilineage plasticity in vitro and in vivo (for review see [23]). In addition, MSCs have a much higher frequency in the adipose tissue (approximately 500-fold more) than in BM [22, 23]. Although both cell populations share many common biological features, certain key differences in surface marker expression between BM-MSCs and ASCs were detected [24, 25]. For instance, while both express the β1 chain of integrins (CD29), only ASCs express CD49d (α4 integrin) [20, 26], which forms a heterodimer with CD29 to create very late activation antigen-4 (VLA-4). This is very interesting in light of the key role of the interaction between VLA-4 and VCAM-1 in the migration of cells into the inflamed CNS in EAE/MS [27]. Finally, several groups, including ours, have found evidence for neural transdifferentiation of ASCs in vitro [28–36], a property which may be relevant for neuroregeneration.

Here we show that the preventive administration of ASCs ameliorated chronic EAE by a dual mechanism, one involving the systemic immune modulation on autoreactive T cells (with a consequent reduction of spinal cord inflammation and demyelination) and one inducing local neurogenesis in inflamed spinal cord, through the secretion of neural growth factors. Most interestingly, ASCs were effective in ameliorating chronic EAE even when administered after disease stabilization, leading to the reduction of CNS inflammation, demyelination, and axonal damage, as well as the increase of endogenous oligodendrocyte precursors.

Materials and Methods

EAE Induction and Treatment Protocols

Chronic EAE was induced in C57Bl/6 female mice 6–8 weeks old (Harlan Italy, San Pietro di Natisone, Italy, http://www.harlan.com) by subcutaneous immunization with 200 μg MOG_{33-35} peptide in incomplete Freund's adjuvant containing 0.8 mg/ml *Mycobacterium tuberculosis* as previously described [37]. Pertussis toxin (50 ng; Sigma-Genosys, Cambridge, U.K., http://www.sigmaaldrich.com/Brands/Sigma_Genosys.html) was injected at the day of immunization and after 48 hours. Body weight and clinical score were blindly registered according to a standard 0–5 scale: 0 = healthy, 1 = limp tail, 2 = ataxia and/or paresis of hindlimbs, 3 = paraplegia, 4 = paraplegia with forelimb weakness or paralysis, 5 = moribund or dead animal. All animals were housed in pathogen-free conditions. The experiments received authorization from the Italian Ministry of Health and were conducted following the principles of the NIH Guide for the Use and Care of Laboratory Animals and the European Community Council (86/609/EEC) directive. To evaluate the clinical and pathological efficacy of ASCs in chronic EAE, cells were administered with two distinct protocols: preventive and therapeutic. In the preventive setting, ASCs (either from wild-type mice or from animals transgenic for green fluorescent protein (GFP)) were injected intravenously at 3 and 8 days postimmunization (dpi), i.e., before the disease onset. In the therapeutic protocol, ASCs were administered intravenously after the peak of disease severity, when the clinical score was stable (23 and 28 dpi). For each injection, 1×10^6 MSC were resuspended in 1 ml phosphate-buffered saline (PBS) without Ca^{2+} and Mg^{2+} and injected through the tail vein; each intravenous administration was divided into two injections of 0.5×10^6 ASC in 0.5 ml vehicle. Control mice received only vehicle.

Mesenchymal Stem Cell Cultures

Murine ASC were obtained from C57Bl/6J (Harlan, Italy, San Pietro di Natisone, Italy) mice 6–8 weeks old, as well as from C57Bl/6-Tg(UBC-GFP)30Scha/J mice (Jackson Laboratories) expressing the GFP fluorescent protein. The isolation of stromal-vascular fraction from adipose tissue was carried out on 10 ml of minced samples obtained from subcutaneous abdominal fat tissue, as previously described [36]. Briefly, after washing in Hank's buffered salt solution, extracellular matrix was digested at 37°C with collagenase and centrifuged at 1,200*g*, and the pellet was resuspended in NH_4Cl; the stromal fraction was then collected by centrifugation and filtration. Murine BM-MSCs were collected by flushing femurs and tibias with medium and filtered as previously described [11, 35]. Cells were then cultured in Dulbecco's modified Eagle medium, glucose, GlutaMAX I™, 15% heat-inactivated adult bovine serum, penicillin, and streptomycin (Invitrogen, Carlsbad, CA, http://www.invitrogen.com). After 72 hours, nonadherent cells were removed. When 70%–80% adherent cells were confluent, they were trypsinized, harvested, and expanded by using culture medium with 50 ng/ml HB-EGF (R&D Systems Inc., Minneapolis, MN, http://www.rndsystems.com). All the experiments were performed using MSCs at 17–23 passages.

MSC Immune Phenotyping and Adhesion Molecules Expression

Murine MSCs were recognized by immune phenotype using monoclonal antibodies (mAbs) specific for CD106 (VCAM-1), CD9, CD44, CD80, CD138, and Sca1. In addition, the absence of hematopoietic markers (CD45, CD11c, and CD34) and endothelial markers (CD31) was assessed as previously described [11]. All mAbs were purchased from BD Pharmingen (San Diego, http://www.bdbiosciences.com/index_us.shtml). We also assessed the expression of platelet-derived growth factor (PDGF) αR on ASCs with a polyclonal antiserum (Sigma), followed by

biotinylated secondary anti-goat IgG and streptavidin-PE. For the study of adhesion molecule expression, ASCs were labeled with fluorescent antibodies for α4 integrins (PS/2 clone, kindly provided by Dr. Eugene Butcher, Stanford University, California, USA), LFA-1 (anti–αL-chain; clone TIB213 from American Type Culture Collection (ATCC), Virginia, USA), PSGL-1 (clone 4RA10, kindly provided by Dr. Dietmar Vestweber, Max Plank Institute, Leipzig, Germany), L-selectin (Mel-14 clone, ATCC), and CD44 (IM/7 clone, ATCC). Isotype-matched antibodies were used as controls. For immune phenotypic analysis, MSCs were detached using trypsin/EDTA (Sigma), washed, and resuspended at 10^6 cells/ml. Cell suspension was incubated with 15% adult bovine serum, followed by incubation with the specific mAbs at 4°C for 30 min. At least 10,000 events were analyzed by flow cytometry (FACScalibur, Becton Dickinson) using the CellQuest software (Becton Dickinson).

ImageStream Data Acquisition and Analysis

ASCs were prepared for immunostaining as described above and then incubated with 10 μg/ml anti–α4 integrin mAb for 30 min on ice. After washing, cells were stained with goat anti-rat IgG-PE conjugated (Invitrogen, San Giuliano Milanese, Italy, http://www.invitrogen.com). Stained cells were resuspended in PBS, and images were acquired on the ImageStream Imaging Cytometer System 100 (Amnis Corporation, Seattle, WA, http://www.amnis.com). Images of fixed cells were collected and analyzed using ImageStream Data Exploration and Analysis Software (IDEAS) [38]. The α4 integrin clustering was evaluated analyzing the distribution on the cells surface of the fluorescence pattern. Uniform (uniform distribution of fluorescence), Clustered (small spots of fluorescence), and Caps (big clusters of fluorescence) cells were gated using the Area feature versus the Delta Centroid (DC) XY feature [39]. The area feature was calculated for channel four (PE-specific emission; area of fluorescence), applying to the images a previously created Threshold mask; this feature allowed us to discriminate between cells with larger fluorescence area (high area values) and smaller fluorescence area. The DC XY feature calculates the distance between the center of the PE fluorescence image and the center of the bright-field image for each image pair. This feature distinguished images with globally distributed staining (lower DC values) from those with capped staining (higher DC values). When plotted versus the Area feature, DC XY permits to distinguish between punctate and uniform staining [39]. Cells with Area values higher than 600 and Radial Delta Centroid values lower than 16 were considered "Uniform"; cells with Area values lower than 600 and Radial Delta Centroid values lower than 16 were considered "Clustered" (small spots of fluorescence). Cells with Radial DC values higher than 16 were considered "Caps" cells (highly polarized fluorescence).

Proliferation Assays

$MOG_{35–55}$–Activated T cells were obtained from draining lymph nodes of mice immunized with antigen as previously described [37]. $CD4^+$ T cells (2×10^5/well) were cocultured with 5,000, 2,000, and 1,000 irradiated ASCs in 96-well microtiter plates in the presence of 30 μg/ml antigen peptide and 8×10^5 APCs (irradiated splenocytes) for 3 days. [^{3}H]-Thymidine (1 mCi) was added in each well 18 hours before the end of cultures. [^{3}H]-Thymidine uptake was determined in a microplate scintillation counter and expressed as counts per minute. In separate experiments we studied the ex vivo proliferation of T cells from peripheral lymph node cells isolated from mice immunized with $MOG_{35–55}$ peptide and treated or not with ASCs. Total draining lymph node cells were isolated both from mice treated with ASCs in the preclinical phase of disease (3 and 8 dpi) and from mice receiving ASCs after disease stabilization (at 23 and 28 dpi). For all ex vivo proliferation experiments, 1×10^6 cells/well were cultured in 96-well microtiter plates in the presence of 10–30 μg/ml MOG peptide or 1 μg/ml anti-CD3 plus 2 μg/well anti-CD28 mAb. After 72 hours of incubation, cultures were pulsed for 18 hours with 1 μCi per well of [H^3]-thymidine, and proliferation was measured from triplicate cultures.

Bio-Plex and ELISA Assays for Cytokines and Growth Factors

Supernatants from lymph node cells isolated from mice treated with ASC in the pre-clinical phase of disease or after disease stabilization, or derived from in vitro co-cultures between $MOG_{35–55}$ activated T-cells and ASC were used for Bioplex cytokine assays (BioRad), following the manufacturer's instructions. Briefly, anti-cytokine conjugated beads were plated in 96-well microtiter plates and then removed by vacuum filtration. Samples were then added, and the plate was incubated for 30 min by mixing at 300 rpm. Bio-Plex cytokine assays were sequentially incubated with the detection antibody and streptavidin-PE; samples were then analyzed immediately by a Bioplex array-system. Unknown cytokine concentrations were automatically calculated by Bio-Plex software using a standard curve derived from a recombinant cytokine standard. To determine the production by ASC of basic fibroblast growth factor (bFGF), brain-derived growth factor (BDNF), ciliary neurotrophic factor, and PDGF-AB, supernatants were obtained from ASCs (3×10^4) in basal condition and after incubation with tumor necrosis factor α (TNF-α) (50 U/ml) for 24 hours and analyzed by Quantikine® ELISA Immunoassay (R&D Systems, Inc.), according to the manufacturer's instructions. Briefly, cells were grown in 24-well plates, and the supernatants were harvested and centrifuged for 10 min to remove cell debris. Samples were added in 96-well precoated plates and incubated for 2 hours at room temperature. After washing, a specific polyclonal antibody followed by substrate solution was added, and the color development was measured at 450 nm on a microplate reader (Bio-Rad, Hercules, CA, http://www.bio-rad.com). The concentration of growth factors was calculated using the standard curve.

Cell Transfection and Biolumiscence In Vivo Imaging

Murine ASCs were transiently transfected with a plasmid encoding for the firefly luciferase (*Photinus pyralis*) under the control of the SV40 early enhancer/promoter region (pGL4.13 internal control vector; Promega, Madison, WI, http://www.promega.com). Transfection was performed by lipofection with the Lipofectamine 2000 reagent system (Invitrogen) according with the manufacturer's instructions; cells were transfected in a 12-well plate (6×10^5 cells/well) and the Lipofectamine/DNA ratio used was 2.5 μl/1 μg. After lipofection, cells were washed and kept for 18 hours at 37°C in complete medium. The transfection efficiency was evaluated by transfecting with the same protocol ASCs with a plasmid encoding for eGFP, under the control of a Cytomegalovirus (CMV) promoter (pEGFP-N1 vector; Clontech, Palo Alto, CA, http://www.clontech.com). Cells were analyzed by flow cytometry for the eGFP fluorescence: efficiency was higher than 55% in all the experiments. The day after transfection, 1.2×10^6 ASCs were transplanted intravenously into healthy or EAE mice (7–9 days after disease onset). For anti–α4 integrin treatment, mice were injected intravenously with 500 μg of anti–α4 integrin mAb every other day, whereas cells were incubated for 30 min on ice before transplantation with 100 μg anti-α4 mAb in 200 μl PBS. Bioluminescent signal generated by luciferase activity was measured using the In Vivo Imaging System IVIS® 200 (Caliper Life Sciences Corporation, Hopkinton, MA, http://www.calipers.com). An aqueous solution of the luciferase substrate D-luciferin (150 mg/kg; Caliper Life Sciences) was injected intravenously 12 min before imaging. Animals were under general anesthesia (2.5% isoflurane in oxygen). Images were acquired using a charge-coupled device camera (acquisition time: 6 min) and analyzed with the Living Image 2.6 software and the Living Image 3D (Xenogen). A pseudocolor image representing light intensity (blue, least intense; red, most intense) was created for each mouse.

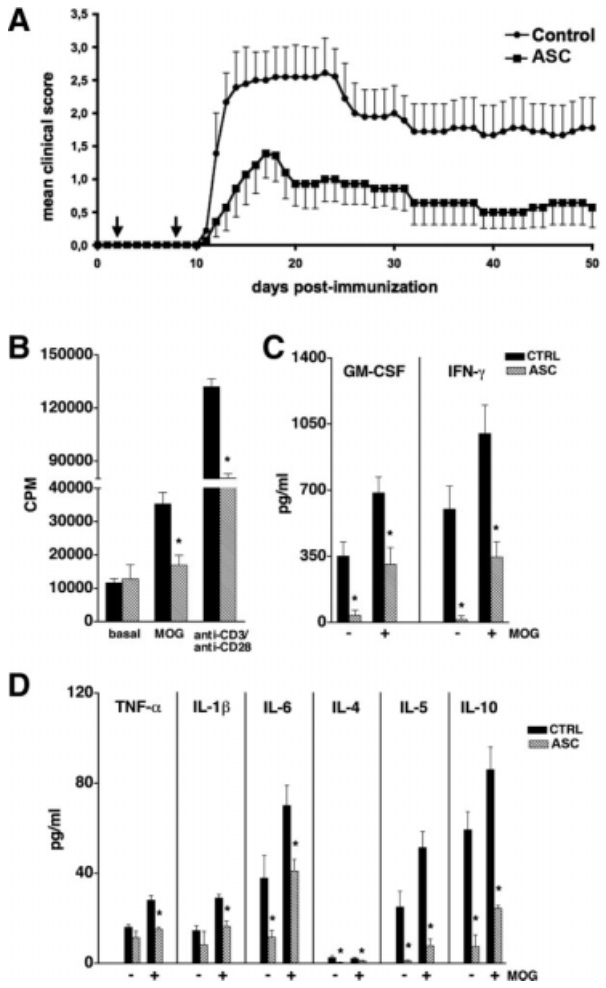

Figure 1. Preventive administration of adipose-derived mesenchymal stem cells (ASCs) inhibits clinical signs of experimental autoimmune encephalomyelitis (EAE) and reduces proliferation and cytokine production of T cells ex vivo. **(A)** Mice were treated with ASC (■) or saline (control; •) during the preclinical phase (3 and 8 days post-injection (dpi)). Daily mean of the clinical scores shows a statistical difference between the two groups of mice starting from 14 dpi. The results from the same experiment are also summarized in Table 1. **(B)** Total draining lymph node cells were isolated from mice transplanted with ASC in the pre-clinical phase of the disease and from control mice. Ex vivo analysis of T-cell proliferation of lymph node cells (1×10^6) after stimulation with the $MOG_{35–55}$ peptide or soluble anti-CD3/anti-CD28 mAbs clearly showed a significant reduction of [^{3}H]-thymidine incorporation in T lymphocytes obtained from mice treated with ASC, in comparison to control (CTRL) EAE animals. Data were obtained from five mice/condition. **C**, **D**. Cytokine production was also modulated in lymph node cells obtained from mice treated with ASC before disease onset and showed a general suppression of cytokine production, in comparison to controls ($p < .02$). Abbreviations: CPM, count per minute; CTRL, control; GM-CSF, granulocyte monocyte colony stimulating factor; IFN-γ, interferon-γ; IL, interleukin; TNF-α, tumor necrosis factor-α.

Intravital Microscopy

ASCs were labeled with green 5-chloromethylfluorescein diacetate (Molecular Probes Inc., Eugene, OR, http://probes.invitrogen.com). To mimic brain inflammation in early phase of EAE, C57Bl/6 female mice were injected intraperitoneally with 12 μg lipopolysaccharide (*Escherichia coli* 026:B6; Sigma-Aldrich) 5–6 hours before the intravital experiment [5, 40]. Previous studies have shown that lipopolysaccharide or TNF administration induces expression of VCAM-1 as well as expression of other adhesion molecules in brain vessels mimicking endothelial activation during EAE [5, 40]. Briefly, animals were anesthetized, and the preparation was placed on an Olympus BX50WI microscope, and a water immersion objective with long focal distance (Olympus Achroplan; Olympus, Tokyo, http://www.olympus-global.com) was used. A total of 1×10^6 fluorescence-labeled cells/condition was slowly injected into the carotid artery by a digital pump. The images were visualized by using a silicon-intensified video camera (VE-1000 SIT; Dage-MTI, Michigan City, IN, http://www.dagemti.com) and recorded using a digital VCR. ASCs that remained stationary on the venular wall for more than 30 s were considered adherent.

Histology and Immunohistochemistry

Frozen sections were obtained from brain, lumbar, dorsal, and cervical spinal cord and processed for hematoxylin and eosin staining, Spielmeyer staining, and immunohistochemistry to evaluate the presence of inflammatory cells, demyelination, axonal loss, and oligodendrocyte progenitors, according to standard protocols and as previously described [41, 42]. For immunohistochemistry, primary antibodies for macrophages/monocytes, CD3, CD4, CD8 T cells (Serotec Ltd., Oxford, U.K., http://www.serotec.com), neurofilaments (Chemicon, Temecula, CA, http://www.chemicon.com), or PDGFαR (Sigma) were used. To evaluate the tissue distribution and the differentiation by GFP-positive ASCs, sections were stained with DAPI and then with anti-CD11b (R&D), CD3, GFAP (Dako), O4 (Chemicon), or PDGFαR mAbs overnight [42, 43]. Slides were viewed under a TCS SP5 confocal scanner (Leica, Heerbrugg, Switzerland, http://www.leica.com). See supporting information for further details concerning the immunohistochemical procedures.

Statistical Analysis

Statistical analysis using a two-tailed Student's *t* test was performed to evaluate differences between ASC-treated and control conditions for several parameters: T cell proliferation, cytokine production, pathological alterations, and number of oligodendrocyte progenitors in EAE lesions.

Results

Preventive Administration of ASC Reduces the Severity of Chronic EAE

Clinical and Neuropathological Effects of ASC-Based Therapy. Control mice developed the first clinical signs of EAE at 12.7 ± 1.3 dpi (mean ± SD), reached a peak at 14.0 ± 1.2 dpi, and then presented a stable disease course, typical of this chronic model (Fig. 1A; Table 1). The pathological analysis of spinal cord sections in all control mice showed the presence of demyelinated areas and inflammatory infiltrates, composed of T lymphocytes and monocyte/macrophages (supporting information). Mice treated with ASCs showed a drastic reduction of the mean clinical scores at disease peak (1.1 ± 0.7 vs. 2.5 ± 0.7 in control mice; $p < .002$) (Table 1), as well as of the areas of inflammation, demyelination, and axonal loss at 50 dpi (Table 1; supporting information). GFP-positive ASCs had similar clinical and pathological effects on EAE as compared with wild-type ASCs (data not shown). No anti-GFP autoreactivity was detected in the serum from ASC-treated EAE animals by immunocytochemistry on GFP-positive ASC cultures (supporting information). In addition, no evidence of GFP reactivity was seen in CD11b-positive macrophages in all EAE lesions examined with both treatment protocols (data not shown).

Table 1. Clinical and pathological features of EAE mice treated with ASCs with preventive (top) and therapeutic (bottom) treatment protocols

Preventive Treatment	Disease onset (dpi)	Mean maximum score	Mean cumulative score	Inflammatory area (%)[a]	Demyelinated area (%)[a]	Axonal loss (%)[b]
Control (10 mice)[c]	12.7 ± 1.3	2.5 ± 0.7	77.9 ± 36.2	18.9 ± 9.5	17.7 ± 8.5	21.8 ± 4.0
ASC (10 mice)[c]	13.7 ± 2.1	1.1 ± 0.7[e]	32.8 ± 21.7[e]	8.4 ± 7.7[f]	9.1 ± 7.6[f]	9.2 ± 5.1[f]
Therapeutic Treatment	**Mean maximum score**	**Mean cumulative score (0–28 dpi)**	**Mean cumulative score (29–72 dpi)**	**Inflammatory area (%)[b]**	**Demyelinated area (%)[b]**	**Axonal loss (%)[c]**
Control (10 mice)[d]	2.2 ± 0.4	25.2 ± 5.3	92.2 ± 25.1	14.2 ± 6.9	14.6 ± 6.6	22.6 ± 6.0
ASC (10 mice)[d]	2.3 ± 0.4	24.8 ± 6.5	63.0 ± 29.6[e]	7.7 ± 2.3[e]	7.1 ± 3.1[e]	3.9 ± 1.1[g]

[a]Percent of the total spinal cord section.
[b]Percent of axonal loss in demyelinated lesions in comparison to normal white matter.
[c]Pathological changes refer to mice sacrificed at 50 dpi.
[d]Pathological changes refer to animals sacrificed at 72 dpi.
[e]$p < .002$.
[f]$p < .0005$.
[g]$p < .02$.
Abbreviations: ASC, adipose-derived mesenchymal stem cell; dpi, days postimmunization; EAE, experimental autoimmune encephalomyelitis.

Mechanisms of the Beneficial Effects of the Preventive Treatment with ASC in EAE

Immune regulation. In agreement with previous results [14], we found that ASCs also inhibited MOG-specific T lymphocyte proliferation both in vitro and ex vivo. In fact, ASCs cocultured in vitro with CD4-positive T cells in the presence of $MOG_{35–55}$ peptide exerted a dose-dependent inhibition of T cell proliferation and induced a significant decrease of interferon γ (IFNγ; supporting information), granulocyte monocyte colony-stimulating factor, IL-17, IL-4, and IL-5 production (data not shown). No effect was observed on the production of TNF-α and IL-1β, which were produced in low amounts after in vitro stimulation with MOG (data not shown). Interestingly, we observed a selective increase of IL-10 production (supporting information), suggesting that ASCs promote the generation of T lymphocytes with regulatory activity in vitro. We next asked whether the effects observed in vitro were also responsible for the in vivo activity of ASCs. Ex vivo analysis of peripheral lymph node cells isolated from mice treated with ASCs showed a significant reduction of proliferation in the presence of $MOG_{35–55}$ when compared with control mice (Fig. 1). In addition, the production of both proinflammatory and anti-inflammatory cytokines by peripheral lymph node cells isolated from mice treated with ASCs and stimulated with $MOG_{35–55}$ was generally suppressed in comparison with control EAE animals (Fig. 1).

ASC and Local Neurogenesis in EAE Lesions. GFP-positive ASCs distributed in normal mice mainly in the spleen and lymph nodes; by contrast, in EAE mice ASCs displayed an increased migration to lymphoid organs but also penetrated into the spinal cord (Fig. 2A), where they persisted up to 93 dpi. In basal conditions, a very limited number of ASCs was found in the submeningeal spaces of both brain and spinal cord (data not shown). In spinal cord from mice with EAE, the vast majority of ASCs was detected mainly within the lesions (Fig. 2C–2F); few GFP-positive ASCs were observed either in regions of normal-appearing white matter.

We then assessed whether ASCs could favor remyelination and regeneration when administered in the preclinical phase of disease. Given the relevance of the PDGF pathway in both oligodendrogenesis and MSC self-renewal [44, 45], we first assessed by flow cytometry the expression of PDGFαR on ASC cultures and found that 28% of them displayed PDGFαR (supporting information). We found that ASC treatment caused local neurogenesis by inducing a threefold increase of PDGFαR-positive oligodendrocyte progenitors (15.0 ± 2.1) when compared with untreated mice (5.4 ± 1.1). We then asked whether the increase in oligodendrocyte progenitors derived from local precursors or from PDGFαR-positive ASCs penetrated into the spinal cord. In this regard, the comparative analysis between the total number of PDGFαR-positive cells and the number of GFP-positive/PDGFαR-positive ASCs showed that approximately 40% of oligodendrocyte precursors derived from ASC (Fig. 2A, 2B), a proportion similar to that found in culture. We next investigated whether GFP-positive ASCs migrated in the parenchyma underwent mature glial differentiation. As summarized in Figure 2B, the double staining with glial phenotypic markers showed that a very limited subset of GFP-positive ASCs displayed mature glial differentiation markers (i.e., GFAP or O4) in EAE lesions. No evidence of binucleated GFP-positive cells expressing such markers was observed in all samples examined (data not shown). Thus, these results suggest that ASCs penetrated and persisted into inflamed spinal cord, where they contributed to activate oligodendroglial progenitors. To better support this point, we then assessed by ELISA assay the secretion by ASCs of growth factors, which may influence their self-renewal as well as the process of oligodendrogenesis. As summarized in Figure 2G, we found that ASCs both in basal conditions and after TNF-α stimulation produced detectable amounts of bFGF, PDGF-AB, and BDNF; no production of ciliary neurotrophic factor was observed in any condition (data not shown).

Therapeutic Administration of ASCs Ameliorates the Severity of Chronic EAE

Clinical and Neuropathological Effects. We then assessed whether ASCs had an effect when injected after the disease entered the chronic phase and the disability is stable. Surprisingly, and in contrast with the results obtained with murine BM-MSCs [14], we found that therapeutic administration of ASCs at 23 and 28 dpi significantly ameliorated the disease severity (Fig. 3; Table 1). The effect was clinically significant at 41 dpi and increased progressively until 72 dpi. The pathological analysis at sacrifice confirmed the beneficial effect of ASCs, in terms of reduction of both demyelination and inflammation (Fig. 3;

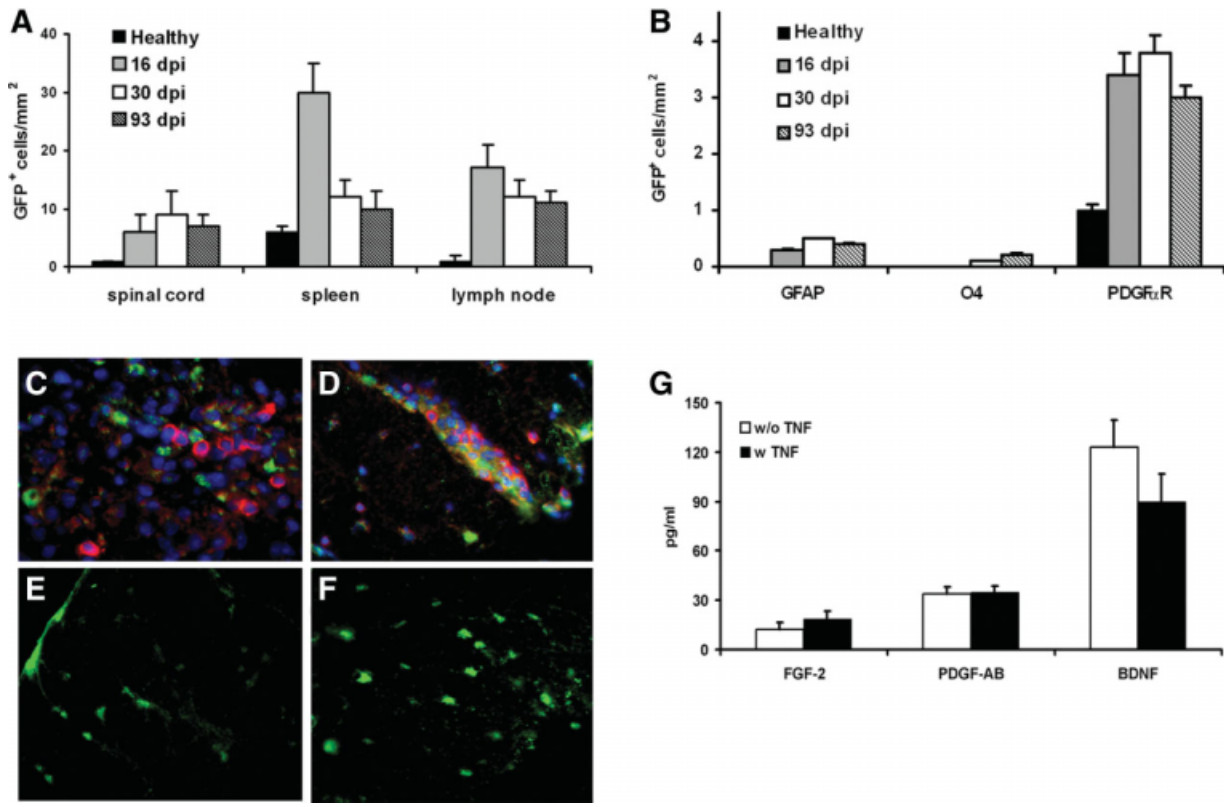

Figure 2. Distribution and differentiation of ASCs injected during the preclinical phase of disease. **(A)** The distribution of green fluorescent protein (GFP)-positive ASCs injected intravenously at 3 and 8 dpi was assessed in lymphoid organs and spinal cord of healthy animals (after 14 days) and EAE mice at several time points. **(B)** The fate of ASCs injected intravenously was assessed with immunofluorescence in the spinal cord of healthy and EAE mice by evaluating the number of GFP-positive cells expressing glial phenotypic markers: GFAP for astrocytes, O4 for mature oligodendrocytes, and PDGFαR for oligodendroglial precursors. **(C, D)** Confocal microscope image with DAPI (blue), CD3 (red), and GFP (green) shows the presence of GFP-positive ASCs in perivascular cuffs in EAE spinal cord at 16 dpi **(C)** and 30 dpi **(D)**. **(E, F)** GFP-positive ASCs are detected in white matter spinal cord at 93 dpi. **(G)** The concentration of bFGF, BDNF, and PDGF-AB was analyzed with ELISA assay in the supernatants of ASCs stimulated (w TNF) or not (w/o TNF) with 50 U/ml TNF-α. Data are expressed as mean ± SD from three different experiments. Abbreviations: BDNF, brain-derived neurotrophic factor; FGF-2, basic fibroblast growth factor; PDGF, platelet-derived growth factor.

Table 1). Strikingly, axonal density in spinal cord of ASC-treated animals was almost comparable to normal mice (Table 1).

Mechanisms of the Beneficial Effects of the Therapeutic Treatment of EAE with ASCs

Immune Regulation. The therapeutic effect of ASCs on established EAE led us to seek the underlying mechanisms of action. Interestingly, homing of ASCs into lymph nodes was lower in mice receiving cells after the disease onset when compared with animals treated in the preclinical phase of the disease. In fact, the number of ASCs injected with the therapeutic protocol detected in lymph nodes was only two times higher than that observed in healthy mice (Fig. 4A) and approximately five times lower than in mice receiving ASCs in the preclinical phase of the disease (Fig. 2A). The proliferation of MOG-specific T cells and the production of proinflammatory cytokines were not different between mice groups at 72 dpi (Fig. 4B). However, basal production of IFNγ by T cells was increased in mice treated with ASCs (Fig. 4C). Importantly, we observed an enhanced production of cytokines IL-4, IL-5, and IL-10 by T cells (Fig. 4D), suggesting that ASCs injected in mice with established disease induce a shift toward a Th2 phenotype contributing to disease amelioration.

ASC Homing to CNS and Induction of Local Neurogenesis in EAE Lesions. In addition to lymphoid organs, the analysis of the distribution of GFP-positive ASCs in spinal cord from EAE mice sacrificed at 72 dpi confirmed the ability of these cells to home into the inflamed CNS when injected in mice with established disease. In this regard, their distribution pattern and quantity (10.1 ± 2.2 GFP-positive cells/mm^2 in EAE lesions) were comparable to those observed with the preventive protocol. To explore the mechanisms sustaining ASC homing to inflamed CNS, we evaluated their adhesion molecule profile. Flow cytometry analysis revealed that α4 integrins were expressed on up to 25% of ASCs, whereas BM-MSCs have no expression of these integrins (supporting information) as previously reported [20, 26]. These results, together with previous data showing that MSCs express β1 integrins, suggest that ASCs express VLA-4 ($\alpha 4\beta 1$) integrin. Moreover, ImageStream analysis revealed that 92% of VLA-4–positive cells express activated VLA-4 (Fig. 5A, 5B). To assess their ability to interact with inflamed brain endothelium, we performed intravital microscopy experiments in an experimental model in which brain endothelium expresses high levels of VCAM-1, the endothelial ligand for VLA-4 integrin [35]. The results confirmed that ASCs were able to efficiently adhere to inflamed brain vessels in vivo (Fig. 5C). To definitively demonstrate that ASCs accumulate in the inflamed brain through a VLA-4–dependent mechanism, we transfected ASCs with luciferase and performed an in vivo bioluminescence assay. The results showed that ASCs accumulate preferentially in spleen and liver in healthy mice, but significantly migrated into inflamed CNS of

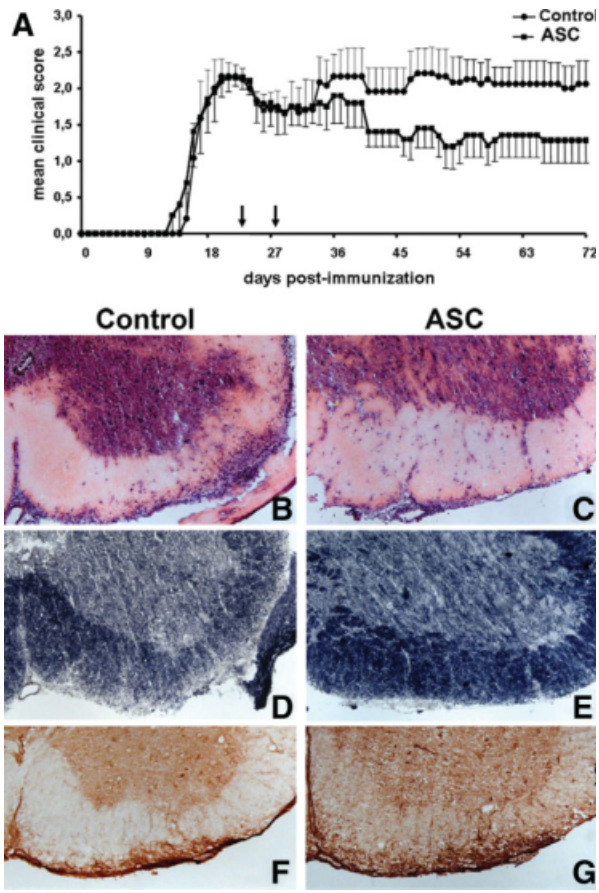

Figure 3. Administration of ASCs in mice with established EAE ameliorates disease course. **(A)** Mice were treated with ASCs (■) or vehicle (control; ●) during the chronic phase of disease (23 and 28 dpi). Daily mean of the clinical scores shows that after approximately 2 weeks ASC-treated animals displayed a significant amelioration of the clinical course in comparison to control EAE mice. Hematoxylin and eosin **(B, C)** and Spielmeyer **(D, E)** staining of lumbar spinal cords confirmed that clinical amelioration was accompanied by a significant reduction of both inflammation and demyelination in ASC-treated animals **(C, E)** in comparison to control mice **(B, D)**. Quantification of these results is summarized in Table 1. **(F, G)** Immunohistochemistry on lumbar spinal cord sections for PDGFαR shows an increase of oligodendrocyte precursors in EAE lesions from ASC-treated mice **(G)** in comparison to control animals **(F)**.

EAE mice, with preferential accumulation in lumbo-sacral spinal cord (Fig. 5D). Interestingly, anti–α4 integrin antibody dramatically inhibited ASC accumulation in inflamed CNS (Fig. 5D).

We next sought for the mechanisms responsible for the therapeutic effect of ASCs. We first evaluated the number of oligodendrocyte precursors, which may contribute to neuroregeneration. As observed in mice receiving ASCs during the preclinical phase of EAE, ASC penetration in EAE lesions induced a three-fold increase of the total number of PDGFαR-positive cells compared with EAE lesions from control mice (Fig. 6A). The comparative analysis of the total number of PDGFαR-positive cells and of GFP-positive/PDGFαR-positive ASCs showed that approximately 20% of oligodendrocyte precursors derived from ASCs (a proportion similar to that expressing PDGFαR on ASCs before injection; supporting information), whereas the majority originated from local precursors (Fig. 6A–6C). As shown for mice treated in the preclinical phase of disease, we observed that a very limited number of GFP-positive cells expressed the markers of mature glial cells (i.e., GFAP or O4) (Fig. 6D, 6E); in particular, mature oligodendrocyte derived from ASCs were less than 2%, suggesting that ASCs do not significantly contribute directly to the process of remyelination. As in preventively ASC-treated mice, no evidence of binucleated GFP-positive cells expressing such markers was observed in all samples examined (data not shown).

Discussion

Stem cells are a promising approach for the treatment of autoimmune diseases of the CNS due to their immune modulatory effects and neuroregenerative potential. NPCs seem to represent the gold standard in chronic EAE, because of their ability to penetrate into the CNS, where they display high neuroregenerative properties as well as anti-inflammatory effects [4, 5]. However, the source and availability of stem cells is becoming a crucial issue for their clinical application. In this regard, previous studies have shown that BM-MSCs were effective in ameliorating both chronic and relapsing-remitting EAE [15, 17, 18]. However, the beneficial effect in chronic EAE was evident only when murine BM-MSCs were injected before disease onset [15]. In both experimental conditions, the main mechanism was related to the immune suppression exerted by murine BM-MSCs on autoreactive B and T cells [15, 17, 24, 25], while their effects within the inflamed CNS are still a matter of debate [15–18]. More recently, also human BM-MSCs have been shown to be effective on chronic EAE by inducing Th2-polarized immune response, reducing IFNγ- and Th17-producing cells, promoting oligodendrogenesis, and inhibiting astrogliosis in EAE [19]. Interestingly, recent data show that BM-MSCs inhibit key mechanisms responsible for EAE induction by a paracrine conversion of CCL2 chemokine from agonist to antagonist of the Th17 cell function [20]. However, although promising results have been previously obtained with BM-MSCs, the invasive nature of BM biopsies may limit their practicality for wider clinical applications. It has been estimated that the frequency of ASCs in collagenase-digested adipose tissue is approximately 500-fold higher that in freshly isolated BM cells [22, 23]. Moreover, the most important features of adipose tissue as a cell source might be the relative expandability of this tissue and the consequent ease with which it can be obtained in relatively large quantities with minimal risk [22].

In the present paper we show that ASCs have a significant beneficial effect on chronic EAE not only when administered in the preclinical phase of disease, but also when injected after disease entered an irreversible clinical course, thus displaying a true therapeutic effect. In both cases, the amelioration of clinical scores was accompanied by a strong reduction of spinal cord inflammation as well as of demyelination and axonal damage in EAE lesions. Our results show that these cells exerted their beneficial effects by acting simultaneously in two distinct sites: lymphoid organs and inflamed CNS. Like BM-MSCs, ASCs induced dramatic changes on antigen-specific T cells in vitro, with dose-dependent inhibition of proliferation and modulation of cytokine secretion [15, 17]. We show that the time of ASC administration is crucial for their homing capacity to lymph nodes with potential implications for the mechanisms of diseases inhibition. The migration to lymph nodes was significantly higher when ASCs were administered shortly after the induction of the autoimmune response, whereas it was lower when administered in mice

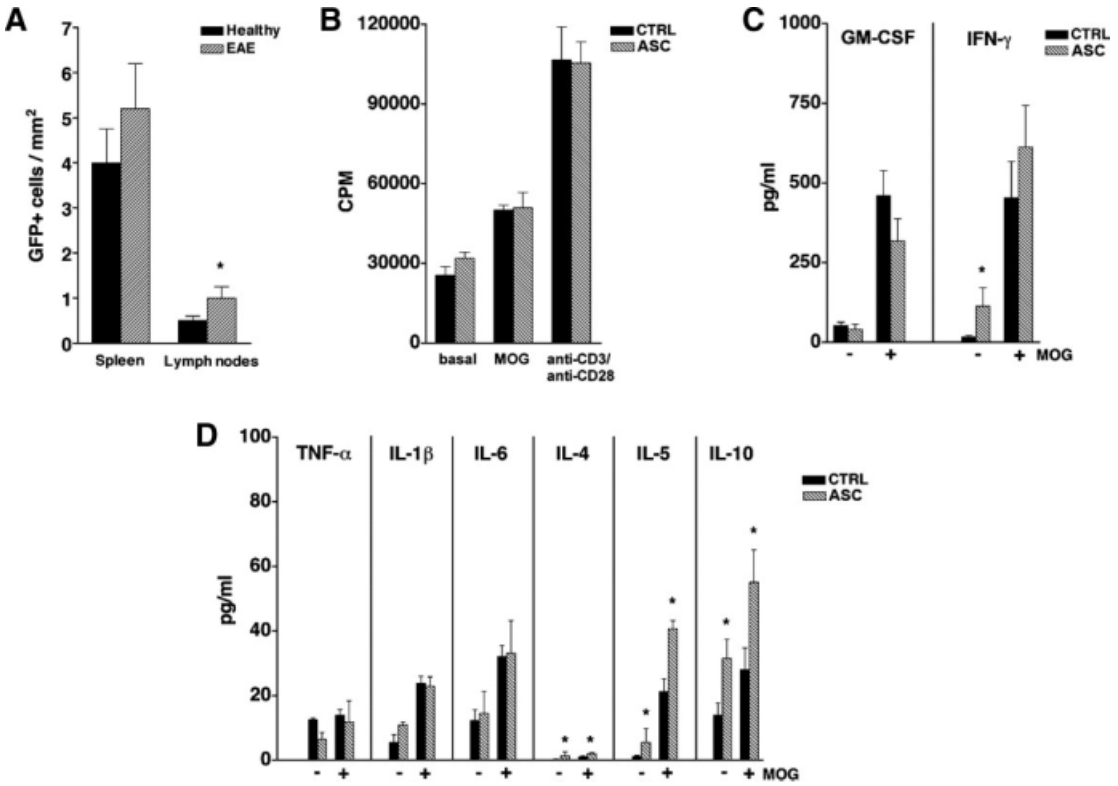

Figure 4. Distribution and functional ex vivo analysis of peripheral lymph node cells isolated from mice treated with ASC during established disease. **(A)** Quantification of GFP-positive ASCs in lymphoid organs from mice treated with ASCs injected at 23 and 28 dpi. Although significantly higher than in healthy mice ($p < .04$), note the low number of cells in the lymph node in comparison to those observed in EAE animals treated with the preventive protocol **(A)**. **(B)** The proliferation of lymph node cells isolated from these mice was not significantly different from control EAE animals. Data were obtained from nine mice/condition. **(C)** Cytokine contents in supernatants of lymph node cells showed that basal production of IFN-γ was increased in cells obtained from ASC-treated mice. **(D)** Interestingly, we observed an enhanced production ($p < .02$) of IL-4, IL-5, and IL-10 by T cells both in the absence and in the presence of antigen, suggesting that ASCs injected in mice with established disease induced a shift toward a Th2 phenotype.

with established disease. This difference may explain the antiproliferative effect and broad inhibition of both pro- and anti-inflammatory cytokine production observed when ASCs were injected in the preclinical phase of disease, but not in mice with established disease. Interestingly, we provided evidence that ASCs injected in mice with established disease induced a Th2-type shift of antigen-specific CD4 T cells in lymph nodes supporting recent results obtained with human BM-MSCs in chronic EAE [19].

The knowledge of the molecular mechanisms controlling ASC-based therapy is of critical importance in the perspective of potential future applications of ASCs in humans. The characterization of the molecular mechanisms involved in the immune modulation and those sustaining ASC homing into the CNS during EAE/MS represent an important contribution to the understanding of ASC tissue-specific delivery. However, the mechanisms involved in the migration of MSCs (of any origin) into the brain are largely unknown. In addition to their immune modulatory activity shared with BM-MSCs, our results suggest that the beneficial effect of ASCs on chronic EAE relies also on the ability to penetrate into the inflamed CNS due to the expression on a significant ASC subset of activated $\alpha 4\beta 1$ integrin, a key adhesion molecule involved in leukocyte and stem cell migration into the inflamed CNS [5, 46]. We demonstrated the presence of activated $\alpha 4$ integrin on a subset of ASCs, which mediated the interaction with inflamed brain endothelium as shown by intravital microscopy experiments. Moreover, in vivo bioluminescence assay showed that ASCs display $\alpha 4$ integrin–dependent migration in inflamed CNS, suggesting that adipose tissue may represent a valuable source of stem cells able to cross the blood–brain barrier and exert their action into the inflamed CNS.

The analysis of distribution of GFP-positive ASCs in EAE mice injected either before or after disease onset indicates that these cells penetrated into the inflamed spinal cord and persisted there up to 3 months, thus suggesting long-lasting effects in target tissues. The persistence of ASCs up to 75 days after intravenous injection has been described in previous studies [47]. In our model, chronic inflammation and expression of VCAM-1 on brain endothelium in MOG-induced EAE may help continuously recruit ASCs expressing $\alpha 4$ integrin from the blood. In addition to promote homing, we speculate that chronic inflammation together with the secretion of growth factors might be responsible for the prolonged survival of ASCs in inflamed spinal cord. These cells in fact produce in basal conditions and after stimulation with TNF-α, bFGF, and PDGF-AB, two factors known to promote MSC self-renewal [48]. In addition to ASCs, activated microglia present in active EAE lesions are known to produce bFGF [49]. From these observations, it is conceivable that the local inflammatory environment supports the prolonged survival of ASCs within EAE lesions.

We then asked whether and how ASCs could have a neuroregenerative effect in EAE spinal cord. In this regard, ASC may participate to remyelination by either differentiating into mature oligodendrocytes able to form new myelin or indirectly by promoting the survival and proliferation of endogenous precursors cells. A direct participation of ASCs to

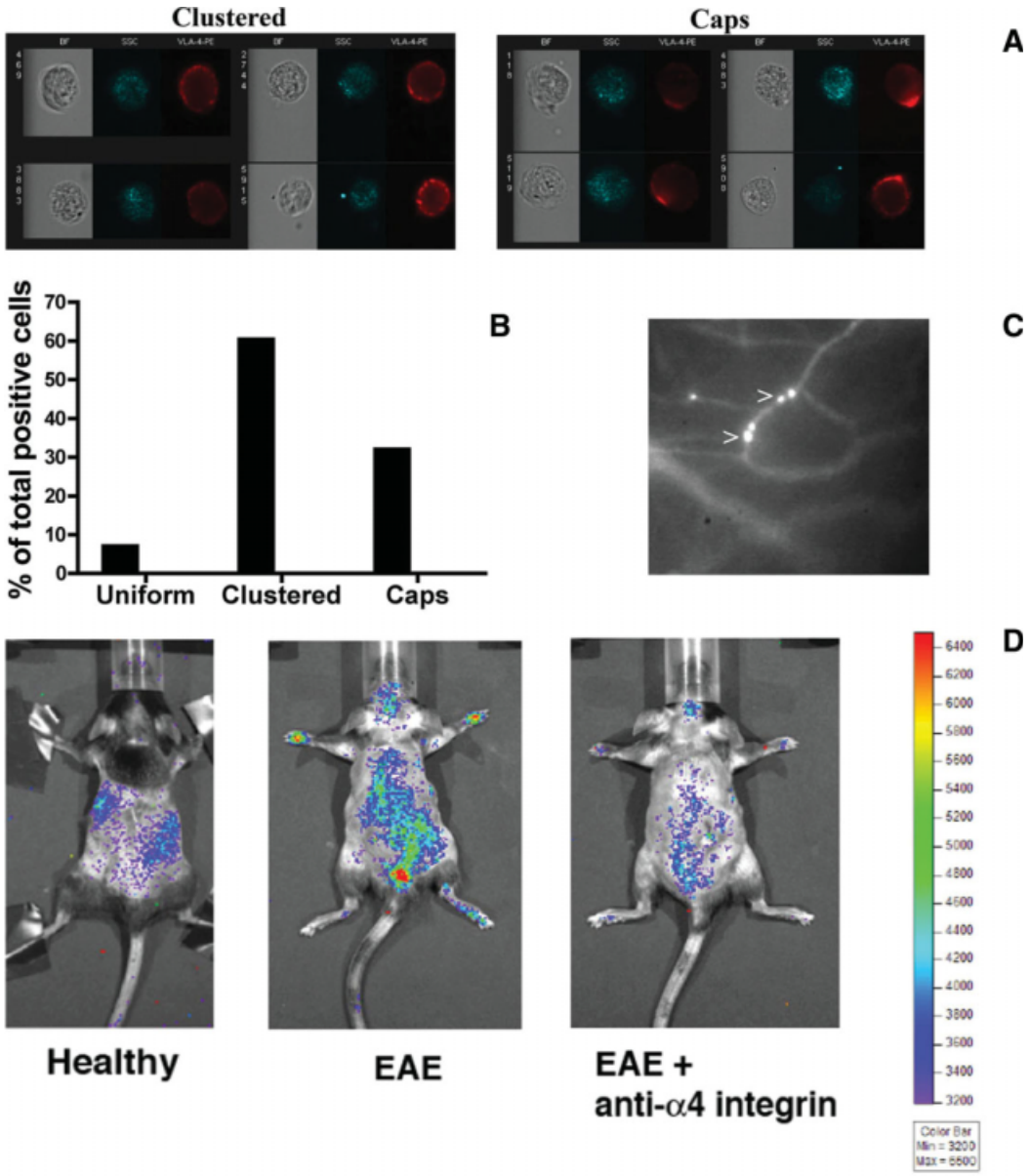

Figure 5. The α4 integrin controls ASC migration into the CNS in EAE mice. **(A, B)** ASCs were stained with anti-α4 integrin antibody followed by anti-rat IgG-PE. Analysis of α4 integrin clustering was evaluated by analyzing the distribution on the cells surface of the fluorescence: Uniform (uniform distribution of fluorescence), Clustered (small spots of fluorescence), and Caps (big clusters of fluorescence). **(A)** Images of eight representative cells: bright-field (BF; white), dark-field/side scatter (SSC; blue), α4 integrin (VLA-4-PE; red). **(B)** Quantification of the three different populations of ASCs according to α4 integrin clustering on the cell surface shows that the vast majority of ASCs display functionally active α4 integrin. **(C)** A micrograph shows fluorescently labeled ASCs arrested in inflamed brain venules in intravital microscopy experiments. Cells are the bright intravascular dots (arrows) inside blood vessels labeled with fluorescent dextrans. **(D)** ASCs transfected with the luciferase reporter gene were transplanted intravenously in healthy or EAE mice (7–9 days after disease onset). Bioluminescent signal by luciferase activity generated by transfected ASCs in transplanted mice was visualized 7 days after ASC injection. Images show the bioluminescent signal detected in one representative animal per group (left: healthy mouse; middle: EAE mouse; right: mouse with EAE + anti-α4 integrin antibody). The color scale next to the images indicates the signal intensity, with red and blue representing high and low signal intensity, respectively. In healthy animals, intravenous injection of ASC results in their accumulation in liver and spleen, whereas in EAE mice the bioluminescent signal is prevalent in areas corresponding to dorsal-lumbar spinal cord. The pretreatment with anti-α4 integrin monoclonal antibody dramatically reduced the signal in these areas.

remyelination seems unlikely because the proportion of GFP-positive cells expressing PDGFαR in EAE lesions of both protocols was comparable to that observed in ASC cultures before injection. Additional evidence against a direct neuroregenerative effect of ASCs came from the analysis of the markers of mature glia expressed by ASCs in situ, which revealed that only a very limited proportion of GFP-positive ASCs acquired the phenotype of mature oligodendroglial cells. In particular, less than 2% of O4-positive oligodendrocytes derived from ASCs at all time points investigated, a proportion that probably do not significantly contribute to the process of remyelination. Although we did not observe any binucleated GFP-positive cells expressing markers of mature glia in our samples, we were not able to establish whether the expression of neural markers on a limited ASC subpopulation in EAE spinal cord reflected a process of true differentiation

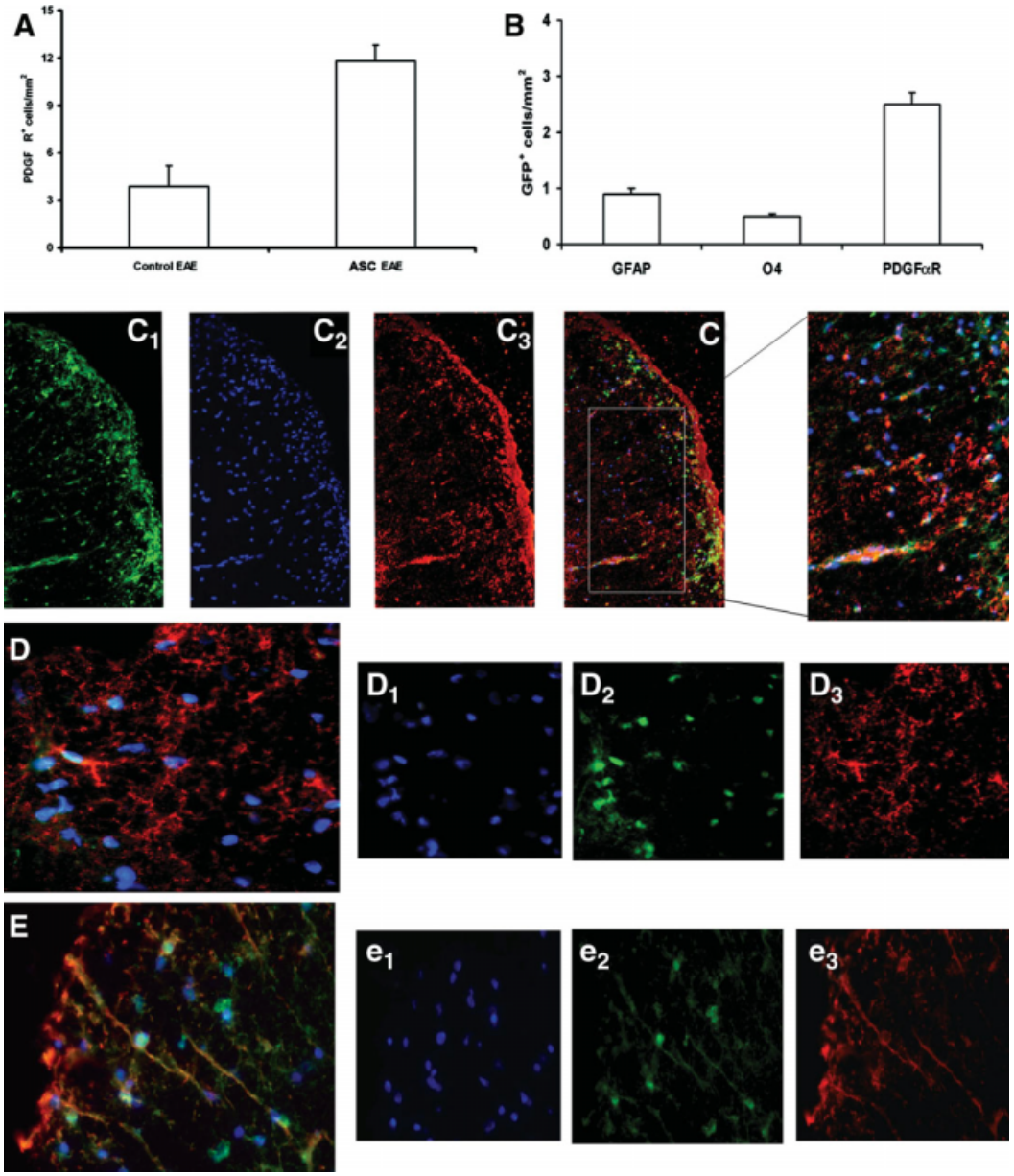

Figure 6. Differentiation of ASCs injected during established disease. **(A)** The number of PDGFα R-positive cells in EAE lesions was significantly increased in animals treated with ASCs with the therapeutic protocol, in comparison to controls at 72 dpi. **(B)** The study of the expression of glial markers on GFP-positive cells in EAE lesions indicate that a subset of ASCs penetrated into the spinal cord expressed PDGFα R-positive, but only a very limited number of ASCs acquired the phenotype of mature GFAP-positive astrocytes or O4-positive oligodendrocytes. In EAE spinal cords from mice injected with GFP-positive ASC at 23 and 28 dpi, a subset of GFP-positive cells (green, **C_1**) expressed PDGFα R (red, **C_3**), as evident in merged image **(C** and **inset)**; nuclei are stained with DAPI (blue, **C_2**). **(D_2, E_2)** In consecutive sections, we show examples of GFP-positive cells expressing the markers of mature O4-expressing oligodendrocytes **(D_3)** or GFAP-positive astrocytes **(E_3)**, visible in merged images **(D, E)**; DAPI staining in **D_1** and **E_1**.

towards a glial phenotype or rather derived from a process of cell fusion, as seen in other experimental conditions [50].

Overall, our results indicate that the main mechanism responsible for the neuroregenerative effect in chronic EAE is a robust activation of endogenous progenitors in EAE lesions, which probably accounted for the process of remyelination. Indeed, the number of endogenous oligodendrocyte precursors (GFP-negative/PDGFαR-positive) was significantly higher in ASC-treated animals in comparison to control EAE. Regarding the molecular mechanism involved in the cross-talk between ASC and oligodendroglial precursors, MSCs are known to produce a variety of neurotrophic factors with relevant effects on NPC proliferation, migration, and differentiation [10, 51–53]. Here we show that ASCs are able to secrete bFGF, PDGF-AB, and BDNF, all factors strongly supporting the process of oligodendrogenic differentiation. In fact, a key role for these factors in the amelioration of EAE observed in our experiments is also suggested by two studies in which the delivery of bFGF or BDNF induced a beneficial effect of clinical and pathological scores in EAE together with an increase of mature oligodendrocytes and their progenitors in an EAE model [54, 55].

In conclusion, our results show that ASCs produce a beneficial effect in chronic EAE by a bimodal mechanism, through

suppression of the autoimmune response in early phases of disease and promotion of Th2-polarized immune response as well as through the induction of local neuroregeneration by endogenous progenitors in animals with established disease. Our data show that ASCs have relevant therapeutic potential in an animal model of chronic MS and might represent a valuable tool for stem cell–based therapy in chronic inflammatory diseases of the CNS. The persistence of ASCs in EAE lesions, together with the beneficial effect displayed in the therapeutic protocol in chronic EAE when clinical and pathological signs are irreversible, may have important implications for the future therapeutic use of ASCs also in other chronic, noninflammatory CNS diseases, where the recruitment of local progenitors is warranted.

Acknowledgments

This work was supported in part by grants from the National Multiple Sclerosis Society, New York, NY (G.C.), Fondazione Cariverona (G.C., B.B., M.K.), Italian Ministry of Education and Research (B.B.), and Fondazione Italiana Sclerosi Multipla (G.C., B.B.).

Disclosure of Potential Conflicts of Interest

The authors indicate no potential conflicts of interest.

References

1 Raine CS. The neuropathology of multiple sclerosis. In: Raine CS, McFarland H, Tourtellotte W, eds. *Multiple sclerosis.* London, UK: Chapman & Hall Med, 1997:149–172.
2 Brex PA, Ciccarelli O, O'Riordan JI et al. A longitudinal study of abnormalities on MRI and disability from multiple sclerosis. N Engl J Med 2002;346:158–164.
3 Trapp BD, Peterson J, Ransohoff RM et al. Axonal transection in the lesions of multiple sclerosis. N Engl J Med 1998;338:278–285.
4 Pluchino S, Quattrini A, Brambilla E et al. Injection of adult neurospheres induces recovery in a chronic model of multiple sclerosis. Nature 2003;422:688–694.
5 Pluchino S, Zanotti L, Rossi B et al. Neurosphere-derived multipotent precursors promote long-lasting neuroprotection by an immunomodulatory mechanism. Nature 2005;436:266–271.
6 Horwitz EM, Le Blanc K, Dominici M et al. Clarification of the nomenclature for MSC: the International Society for Cellular Therapy position statement. Cytotherapy 2005;7:393–395.
7 Erices A, Conget P, Minguell JJ. Mesenchymal progenitor cells in human umbilical cord blood. Br J Haematol 2000;109:235–242.
8 Jiang Y, Vaessen B, Lenvik T et al. Multipotent progenitor cells can be isolated from postnatal murine bone marrow, muscle, and brain. Exp Hematol 2002;30:896–904.
9 Zuk PA, Zhu M, Mizuno H et al. Multilineage cells from human adipose tissue: implications for cell-based therapies. Tissue Eng 2001;7:211–228.
10 Munoz JR, Stoutenger BR, Robinson AP et al. Human stem/progenitor cells from bone marrow promote neurogenesis of endogenous neural stem cells in the hippocampus of mice. Proc Natl Acad Sci USA 2005;102:18171–18176.
11 Krampera M, Glennie S, Dyson J. Bone marrow mesenchymal stem cells inhibit the response of naive and memory antigen-specific T cells to their cognate peptide. Blood 2003;101:3722–3729.
12 Uccelli A, Moretta L, Pistoia V. Immunoregulatory function of mesenchymal stem cells. Eur J Immunol 2006;36:2566–2573.
13 Uccelli A, Moretta L, Pistoia V. Mesenchymal stem cells in health and disease. Nat Rev Immunol 2008;8:726–736.
14 Cui L, Yin S, Liu W et al. Expanded adipose-derived stem cells suppress mixed lymphocyte reaction by secretion of prostaglandin E2. Tissue Eng 2007;13:1185–1195.
15 Zappia E, Casazza S, Pedemonte E et al. Mesenchymal stem cells ameliorate experimental autoimmune encephalomyelitis inducing T-cell anergy. Blood 2005;106:1755–1761.
16 Zhang J, Li Y, Chen J et al. Human bone marrow stromal cell treatment improves neurological functional recovery in EAE mice. Exp Neurol 2005;195:16–26.
17 Gerdoni E, Gallo B, Casazza S et al. Mesenchymal stem cells effectively modulate pathogenic immune response in experimental autoimmune encephalomyelitis. Ann Neurol 2007;61:219–227.
18 Kassis I, Grigoriadis N, Gowda-Kurkalli B Et al. Neuroprotection and immunomodulation with mesenchymal stem cells in chronic experimental autoimmune encephalomyelitis. Arch Neurol 2008;65:753–761.
19 Bai L, Lennon DP, Eaton V et al. Human bone marrow-derived mesenchymal stem cells induce Th2-polarized immune response and promote endogenous repair in animal models of multiple sclerosis. Glia 2009;57:1192–1203.
20 Rafei M, Campeau PM, Aguilar-Mahecha A et al. Mesenchymal stromal cells ameliorate experimental autoimmune encephalomyelitis by inhibiting CD4 Th17 T cells in a CC chemokine ligand 2-dependent manner. J Immunol 2009;182:5994–6002.
21 De Ugarte DA, Alfonso Z, Zuk PA et al. Differential expression of stem cell mobilization-associated molecules on multi-lineage cells from adipose tissue and bone marrow. Immunol Lett 2003;89:267–270.
22 Fraser JK, Wulur I, Alfonso Z et al. Fat tissue: an underappreciated source of stem cells for biotechnology. Trends Biotechnol 2006;24:150–154.
23 Parker AM, Katz AJ. Adipose-derived stem cells for the regeneration of damaged tissues. Expert Opin Biol Ther 2006;6:567–578.
24 Puissant B, Barreau C, Bourin P et al. Immunomodulatory effects of human adipose tissue-derived stem cells: comparison with bone marrow mesenchymal stem cells. Br J Haematol 2005;129:118–129.
25 McIntosh K, Zvonic S, Garrett S et al. The immunogenicity of human adipose-derived cells: temporal changes in vitro. Stem Cells 2006;24:1246–1253.
26 Gronthos S, Franklin DM, Leddy HA et al. Surface protein characterization of human adipose tissue-derived stromal cells. J Cell Physiol 2001;189:54–63.
27 Constantin G, Majeed M, Giagulli C et al. Chemokines trigger immediate beta2 integrin affinity and mobility changes: differential regulation and roles in lymphocyte arrest under flow. Immunity 2000;16:759–769.
28 Safford KM, Hicok KC, Safford SD et al. Neurogenic differentiation of murine and human adipose-derived stromal cells. Biochem Biophys Res Commun 2002;294:371–379.
29 Safford KM, Safford SD, Gimble JM et al. Characterization of neuronal/glial differentiation of murine adipose-derived adult stromal cells. Exp Neurol 2004;187:319–328.
30 De Ugarte DA, Morizono K, Elbarbary A et al. Comparison of multilineage cells from human adipose tissue and bone marrow. Cells Tissues Organs 2003;174:101–109.
31 Kang SK, Shin MJ, Jung JS et al. Autologous adipose tissue-derived stromal cells for treatment of spinal cord injury. Stem Cells Dev 2006;15:583–594.
32 Kokai LE, Rubin JP, Marra KG. The potential of adipose-derived adult stem cells as a source of neuronal progenitor cells. Plast Reconstr Surg 2005;116:1453–1460.
33 Fujimura J, Ogawa R, Mizuno H et al. Neural differentiation of adipose-derived stem cells isolated from GFP transgenic mice. Biochem Biophys Res Commun 2005;333:116–121.
34 Ning H, Lin G, Lue TF et al. Neuron-like differentiation of adipose tissue-derived stromal cells and vascular smooth muscle cells. Differentiation 2006;74:510–518.
35 Krampera M, Marconi S, Pasini A et al. Induction of neural-like differentiation in human mesenchymal stem cells derived from bone marrow, fat, spleen and thymus. Bone 2007;40:382–390.
36 Anghileri E, Marconi S, Pignatelli A et al. Neuronal differentiation potential of human adipose-derived mesenchymal stem cells. Stem Cells Dev 2008;17:909–916.
37 Constantin G, Laudanna C, Brocke S et al. Inhibition of experimental autoimmune encephalomyelitis by a tyrosine kinase inhibitor. J Immunol 1999;162:1144–1149.
38 George TC, Fanning SL, Fitzgerald-Bocarsly P et al. Quantitative measurement of nuclear translocation events using similarity analysis of multispectral cellular images obtained in flow. J Immunol Methods 2006;311:117–125.
39 Bolomini-Vittori M, Montresor A, Giagulli C et al. Regulation of conformer-specific activation of the integrin LFA-1 by a chemokine-triggered Rho signaling module. Nat Immunol 2009;10:185–194.
40 Piccio L, Rossi B, Scarpini E et al. Molecular mechanisms involved in lymphocyte recruitment in brain microcirculation: critical roles for PSGL-1 and trimeric G alpha-linked receptors. J Immunol 2002;168:1940–1949.
41 Lovato L, Cianti R, Gini B et al. Transketolase and CNPase I are specifically recognized by IgG autoantibodies in multiple sclerosis patients. Mol Cell Proteomics 2008;7:2337–2349.

42 Lolli F, Mulinacci B, Carotenuto A et al. An N-glucosylated peptide detecting disease-specific autoantibodies, biomarkers of multiple sclerosis. Proc Natl Acad Sci USA 2005;102:10273–10278.
43 Bonetti B, Pohl J, Gao YL et al. Cell death during autoimmune demyelination: effector but not target cells are eliminated by apoptosis. J Immunol 1997;159:5733–5741.
44 Tokunaga A, Oya T, Ishii Y et al. PDGF receptor beta is a potent regulator of mesenchymal stromal cell function. J Bone Mineral Res 2008;23:1519–1528.
45 Lachapelle F, Avellana-Adalid V, Nait-Oumesmar B, Baron-Van Evercooren A. Fibroblast growth factor-2 and platelet-derived growth factor AB promote adult SVZ-derived oligodendrogenesis in vivo. Mol Cell Neurosci 2002;20:390–403.
46 Yednock TA, Cannon C, Fritz LC et al. Prevention of experimental autoimmune encephalomyelitis by antibodies against alpha 4 beta 1 integrin. Nature 1992;356:63–66.
47 Meyerrose TE, De Ugarte DA, Hofling AA et al. In vivo distribution of human adipose-derived mesenchymal stem cells in novel xenotransplantation models. Stem Cells 2007;25:220–227.
48 Zaragosi LE, Ailhaud G, Dani C. Autocrine fibroblast growth factor 2 signaling is critical for self-renewal of human multipotent adipose-derived stem cells. Stem Cells 2006;24:2412–2419.
49 Liu X, Mashour GA, De Webster H, Kurtz A. Basic FGF and FGF receptor 1 are expressed in microglia during experimental autoimmune encephalomyelitis: temporally distinct expression of midkine and pleiotrophin. Glia 1998;24:390–397.
50 Spees JL, Olson SD, Ylostalo J et al. Differentiation, cell fusion and nuclear fusion during ex vivo repair of epithelium by human adult stem cells from bone marrow stroma. Proc Natl Acad Sci USA 2003; 100:2397–2402.
51 Caplan A, Dennis JE. Mesenchymal stem cell as trophic mediators. J Cell Biochem 2006;98:1076–1084.
52 Rivera FJ, Couillard-Despres S, Pedre X et al. Mesenchymal stem cells instruct oligodendrogenic fate decision on adult neural stem cells. Stem Cells 2006;24:2209–2219.
53 Goddard DR, Berry M, Butt AM. In vivo actions of fibroblast growth factor 2 and insulin-like growth factor I on oligodendrocyte development and myelination in the central nervous system. J Neurosci Res 1999;57:74–85.
54 Ruffini F, Furlan R, Poliani PL et al. Fibroblast growth factor 2 gene therapy reverts the clinical course and the pathological signs of chronic experimental autoimmune encephalomyelitis in C57BL/6 mice. Gene Therapy 2001;8:1207–1213.
55 Makar TK, Bever CT, Singh IS et al. Brain-derived neurotrophic factor gene delivery in an animal model of multiple sclerosis using bone marrow stem cells as a vehicle. J Neuroimmunol 2009;210:40–51.


See www.StemCells.com for supporting information available online.